Journal of Geography and Geology; Vol. 10, No. 3; 2018
ISSN 1916-9779 E-ISSN 1916-9787
Published by Canadian Center of Science and Education

A Spectral Analysis of Snow in Mt. Rainier

Shrinidhi Ambinakudige[1], Pushkar Inamdar[2] & Aynaz Lotfata[1]

[1] Mississippi State University, USA

[2] University of California San Francisco, USA

Correspondence: Shrinidhi Ambinakudige, Department of Geosciences, Mississippi State University, USA. E-mail: ssa60@msstate.edu

Received: July 25, 2018 Accepted: August 4, 2018 Online Published: August 11, 2018

doi:10.5539/jgg.v10n3p20 URL: http://dx.doi.org/10.5539/jgg.v10n3p20

Abstract

Snow cover helps regulate the temperature of the Earth's surface. Snowmelt recharges groundwater, provides run-off for rivers and creeks, and acts as a major source of local water for many communities around the world. Since 2000, there has been a significant decrease in the snow-covered area in the Northern Hemisphere. Climate change is the major factor influencing the change in snow cover amount and distribution. We analyze spectral properties of the remote sensing sensors with respect to the study of snow and examine how data from some of the major remote sensing satellite sensors, such as (Advanced Spaceborne Thermal Emission and Reflection Radiometer) ASTER, Landsat-8, and Sentinel-2, can be used in studying snow. The study was conducted in Mt. Rainier. Although reflectance values recorded were lower due to the timing of the data collection and the aspect of the study site, data can still be used calculate normalized difference snow index (NDSI) to clearly demarcate the snow from other land cover classes. NDSI values in all three satellites ranged from 0.94 to 0.97 in the snow-covered area of the study site. Any pollutants in snow can have a major influence on spectral reflectance in the VIS spectrum because pollutants absorb more than snow.

Keywords: remote sensing, spectral, snow, cryosphere

1. Introduction

Snow cover is the most significant component of the cryosphere, and it currently covers a mean winter maximum of 47 million square kilometers (NSDIC 2018). Snow cover helps keep the Earth’s radiation budget in balance by regulating the temperature of the Earth's surface (Dietz et al. 2012). High snow reflectance helps to cool the planet (NSDIC 2018). In addition, snowmelt recharges groundwater, provides run-off for rivers and creeks, and acts as a major source of local water for many communities around the world (Jain et al. 2008). Since 2000, the snow-covered area has decreased in the Northern Hemisphere, especially during the spring snowmelt season (Kunle; et al. 2016, Rutgers University Global Snow Lab 2017). Climate change is the major factor influencing the change in snow cover amount and distribution, and it can cause earlier spring melts and shorter snow cover seasons (NSDIC 2018). Therefore, measuring and monitoring the snow cover extent is essential for climate change studies as well as for ground and surface water management planning purposes.

Remote Sensing satellite images, such as the Moderate Resolution Imaging Spectroradiometer (MODIS), Landsat-8, and Advanced Very High Resolution Radiometer (AVHRR) and many more provide a useful measurement of snow cover. Snow grain size and shape, water content, snow depth, snow impurities, and temperature influence snow reflectivity and scattering characteristics (Domine et al. 2007). Consequently, the remote sensing sensor type, resolution, and interference of all these factors vary the retrieval of snow parameters.

Snow has very high albedo in the visible (VIS) spectrum (Rees 2006; Ambinakudige and Joshi 2012). Snow can reflect 80-97% of the radiation in the VIS spectrum, depending on the presence of impurities, grain size, and age of the snow (Ambinakudige and Joshi 2012; Pellika and Rees 2006). As snow ages, the percentage of reflected insolation decreases. In the long wavelength spectrum, the reflectance of snow declines significantly, reaching near-zero values in the near-infrared (NIR) region (Wang et al. 2005). Besides, different grain sizes lead to high variability in the reflection properties of snow (Dozier 1989). In the VIS spectrum, the differences of the snow signatures are small, but in the longer wavelengths (from 0.95 to 1.40 μm), the differences increase (Rees 2006). It is important to understand how various pollutants (e.g., black carbon, dust, algae) influence snow albedo (Warren 2013).

Multispectral remote sensing sensors on satellites are powerful tools to measure and monitor changes in the status of the cryosphere (Rees 2006; Ambinakudige and Joshi 2012). In recent years, new waves of multispectral satellite data were made available, including Landsat-8 OLI and Sentinel-2 satellite data.

There are two main objectives of this study. First, we analyze how spectral properties of the sensors limit or enhance their performance in the study of the cryosphere. Second, we investigate the extent of information available from full-spectrum data that can be used to examine how data from some of the major remote sensing satellite sensors, such as ASTER, Landsat-8, and Sentinel-2, can be used in studying snow.

2. Study Area

The field data were collected on Mt. Rainier, which is in the State of Washington (Figure 1). Mt. Rainier is the highest mountain in the Cascade Range of the Pacific Northwest. It is an active stratovolcano located in the Mount Rainier National Park. There are 25 major glaciers and numerous unnamed snowfields on Mt. Rainier. It has about a quarter of the total ice area in the lower 48 states (Meier 1998). The mountain, an essential water source, supports six major river systems. The glaciers on the north aspect of Mount Rainier are generally larger and have more volume (Driedger and Kennard 1986). Glaciers and perennial snowfields account for approximately 8.5% of the total area of Mount Rainier National Park (Beason 2017).

Figure 1. The study area – Mt. Rainier. Image Source: ESRI – ARGGIS Online

3. Method

We collected in situ reflectance data using an Analytical Spectral Devices (ASD) Field-SpecPro spectroradiometer to investigate the extent of information available from full-spectrum data and to examine how data from some of the major remote sensing satellite sensors can be used in studying snow. This analysis can help researchers understand how spectral and radiometric properties of the sensors limit or enhance their performance in the study of the cryosphere. For this study, visible through shortwave infrared (350–2500 nm), reflectance data were collected during a field campaign at the Paradise on Mt. Rainer, Washington, on May 4, 2016. By the end of April 2016, Mt. Rainer had received about 1,744.98 cm of snow for that season (about 1,722.92 cm fell in the year 2015-2016).

We collected over 150 points of spectral data for three different snow types: clean, firm, and dirty snow. We considered snow with very minimum or no dust as clean snow. We did not measure the snow grain size. Because there were no new snowfalls for the month prior to the fieldwork date in the study area, there was no fresh snow on the ground. In those areas of the study site that were used heavily by skiers and general visitors, there was substantial dust and other impurities in the snow.

While collecting the reflectance data, we ensured that the measurements were made perpendicular to the solar azimuth and without any objects present that might scatter the radiation. We held the probe at arm's length to one side to avoid any scattered radiation from our clothes that might affect the readings. Also, walking either up or

down sun is recommended to reduce error while collecting the data. The rule of thumb in spectral data collection is to record data within ± two hours of solar noon and the sun's zenith angle of lower than 43.5 degrees (Goetz 2012). Nevertheless, we collected the data starting at 3:20 p.m., which affected the rate of reflectance from the snow surface.

4. Results

The spectroradiometer readings were grouped into wavelengths covering different bands of ASTER, Landsat-8 OLI, and Sentinel-2 satellites (Table 1). These are some of the most commonly used satellite images to study the cryosphere. The ASTER has 14 bands. Bands 1-3 cover the Visible and Near-Infrared (VNIR) area, bands 4-9 cover the Shortwave Infrared (SWIR) area, and bands 10-14 cover the thermal infrared area. For our analysis, we averaged the reflectance values of wavelengths that covered each band. Similarly, the Landsat-8 OLI has 11 bands, and the Sentinel-2 has 12 bands covering different parts of the spectrum useful for cryosphere studies (Table 1).

Reflectance data recorded by the spectroradiometer were then averaged for the wavelength bands of the Landsat-8 (Figure 2a), ASTER (Figure 2b), and Sentinel-2 (Figure 2c) satellites. Typical spectral signatures of fine snow, coarse snow, and medium-sized snow provided by the ECOSTRESS Spectral Library–Version 1.0 are also shown in Figure 2d17.

In the Landsat-8 data, bands 1 through 5 covering VNIR areas had a higher reflectance in all three snow types. In the ASTER data, bands 1 through 3 covering VNIR areas were useful for remote sensing of snow. The Sentinel-2 satellite has bands 1 through 9 that can be used in snow mapping, giving higher spectral as well spatial resolutions for snow cover mapping.

Figure 2d shows the spectral signatures of three types of snow: fine-grain snow, coarse-grain snow, and medium-grain snow. The reflectance values recorded by the spectroradiometer shown in Figures 2a, 2b, and 2c have similar trends to the one shown in Figure 2d. However, the recorded reflectance values are lower compared to the reflectance values shown in Figure 2d.

Table 1. Spectral Bands of Aster, Landsat-8 OLI and Sentinel-2 satellites

	Aster Bands				Landsat Bands				Sentinel-2 Bands		
Band	Spectrum Covered	Wave-lengths (μm)	Resolu-tion (m)	Bands	Spectrum Covered	Wave-lengths (μm)	Resol-ution (m)	Bands	Spectrum Covered	Central Wavelength (μm)	Resol-ution (m)
1	VNIR	0.520- 0.600	15	1	Ultra-Blue	0.433–0.453	30	1	Coastal aerosol	0.443	60
2	VNIR	0.630- 0.690	15	2	Blue	0.450–0.515	30	2	Blue	0.490	10
3N	VNIR	0.760- 0.860	15	3	Green	0.525–0.600	30	3	Green	0.560	10
3	VNIR	0.760- 0.860	15	4	Red	0.630–0.680	30	4	red	0.665	10
4	SWIR	1.600- 1.700	30	5	NIR	0.845–0.885	30	5	Vegetation Red Edge	0.705	20
5	SWIR	2.145-2.185	30	6	SWIR	1.560–1.660	30	6	Vegetation Red Edge	0.740	20
6	SWIR	2.185- 2.225	30	7	SWIR	2.100–2.300	30	7	Vegetation Red Edge	0.783	20
7	SWIR	2.235- 2.285	30	8	Pan	0.500–0.680	15	8	NIR	0.842	10
8	SWIR	2.295- 2.365	30	9	Cirrus	1.360–1.390	30	8A	Vegetation Red Edge	0.865	20
9	SWIR	2.360- 2.430	30	10	TIR	10.60-11.20	100	9	Water Vapor	0.945	60
10	TIR	8.125- 8.475	90	11	TIR	11.50-12.50	100	10	SWIR- Cirrus	1.375	60
11	TIR	8.475- 8.825	90					11	SWIR	1.610	20
12	TIR	8.925- 9.275	90					12	SWIR	2.190	20
13	TIR	10.25-10.95	90								
14	TIR	10.95–11.65	90								

There are several reasons for the lower reflectance values in our study. The data were collected at 3:20 p.m. until about 5 p.m. However, the recommended time frame for collecting reflectance data is ± 2 hours from solar noon (or local noon). When collecting reflectance in a mountainous area, the aspect of the mountain affects the percent of reflectance. In our study, the unfavorable aspect and the time of collection resulted in a low reflectance recording in all snow cover types. Because the reflectance data we collected were low in all land cover types, including bare earth and vegetation (not shown in this paper), the reduction in reflectance was proportional to the land cover type's reflectance in an ideal condition. Therefore, even though the data were not collected under favorable conditions, they are useful in snow cover mapping. To use the data more efficiently and improve the accuracy of snow cover mapping, we employed a derived index instead of the raw readings. Therefore, we calculated the

Normalized Difference Snow Index (NDSI) instead of relying entirely on reflections recorded by individual bands.

NDSI is the commonly used index to map snow cover. The index creates a contrast between two bands with very different reflectance characteristics, which can help to discriminate between snow, ice, and cloud. The reflectance of new or old snow with fine, medium, or coarse granular size at longer wavelengths has low to extremely low albedo measurements. The decline of snow reflectance in the SWIR region can be useful to distinguish between cloud and snow because clouds reflect a higher proportion of SWIR18, 19. This can create a large contrast when compared to wavelengths in the VIS region.

NDSI is calculated using (Green – SWIR)/(Green + SWIR)8. The red band instead of the green band has also been used in NDSI calculation20; however, we adopted the traditional method and used green and SWIR bands. While snow absorbs in the SWIR region (e.g., at 1.6 mm), it reflects in the VIS region (e.g., at 0.66 mm). NDSI can show a contrast between pixels with snow and pixels without snow.

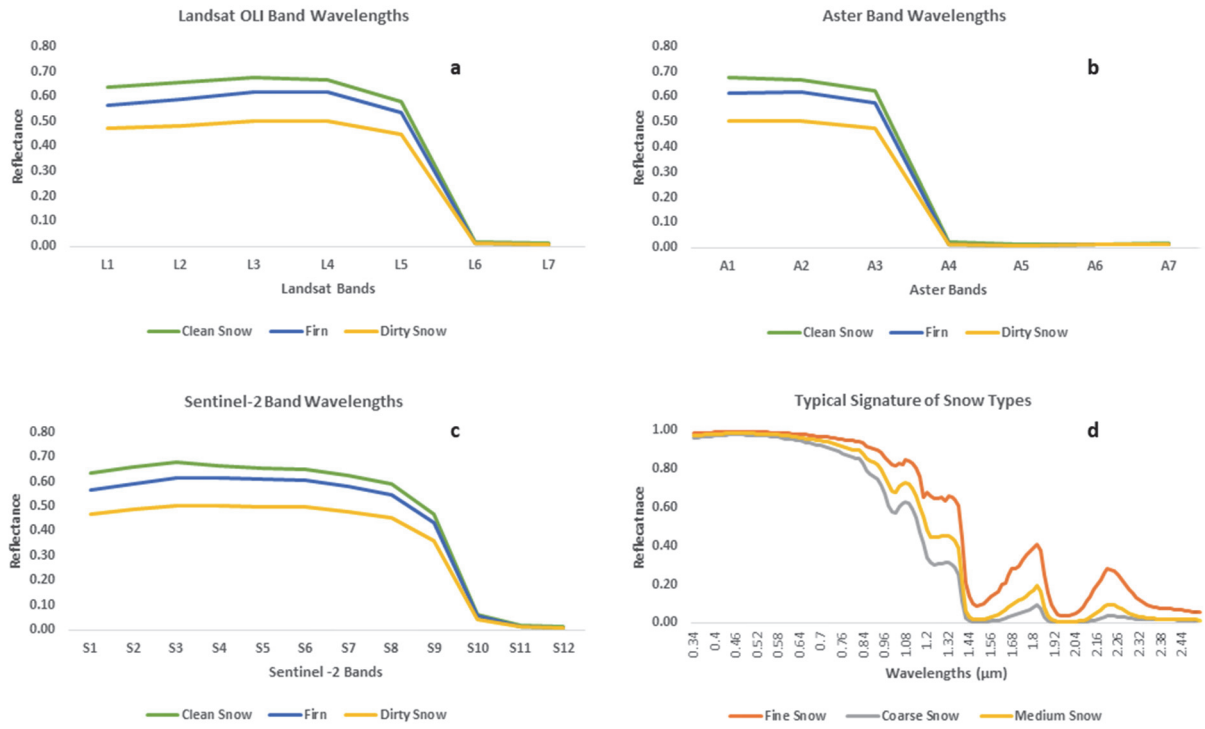

Figure 2. The spectral reflectance of snow types

In ASTER data, bands 3 and 4 can be used to calculate NDSI. Cloud and snow reflectances are similar in band 3 but different in the infrared region. In band 4, the reflectance of clouds is very high but low for snow. In the Landsat-8 data, bands 3 and 6 are used in the NDSI calculation. In the Sentinel-2 data, bands 3 and 11 can be used in the NDSI calculation. We can use snow/ice thresholds of ≥ 0.4 (low confidence) 18, ≥ 0.5 (medium confidence), and/or ≥ 0.6 for higher confidence.

In our study, although reflectance values recorded were lower due to the timing of the data collection and the aspect of the study site, data can still be used calculate NDSI to clearly demarcate the snow from other land cover classes. NDSI values in all three satellites ranged from 0.94 to 0.97 in the snow-covered areas of the study site.

5. Conclusion

In this paper, we analyzed the reflectance values recorded in three types of snow in Mt. Rainier. Our reflectance values were significantly lower than the typical reflectance value in snow (Figure 2), but can be used in calculating NDSI and measure the snow cover extent. The reflectance value recorded in a sensor depends on the angle of incidence, slope of ground, time of year and time of day, and sun azimuth. Dirt and pollutants, such as dust and soot, can considerably modify snow spectral reflectance in the VIS and NIR regions (Kokhanovsky 2013). In pure snow, absorption is very weak in the VIS and NIR regions. Any pollutants in snow can have a major influence on spectral reflectance in the VIS spectrum because pollutants absorb more than snow. Researchers (Hadley and

Kirchstetter 2012) have shown up to a 20% decrease in snow albedo for the soot concentration of about 1.68μg g^{-1} of snow. Painter et al. (2009) found that the reflectance of snow at 412 nm is reduced by 50% when the dust with c = 0.37 mg g^{-1} was deposited on a snow layer. Reflectance is also reduced due to the presence of algae. Takeuchi et al. (2006) reported a 25% decrease in snow reflectance at 412 nm due to the presence of red snow algae.

References

Ambinakudige, S., & Joshi, K. (2102). *The Remote Sensing of Cryosphere*. In *Remote Sensing - Applications,* Dr. Boris Escalante (Ed.), InTech. ISBN: 978-953-51-0651-7.

Baldridge, A. M., Hook, S. J., Grove, C. I., & Rivera, G. (2009). The ASTER Spectral Library Version 2.0. *Remote Sensing of Environment, 113*, 711-715.

Beason, S. R. (2017). *Change in glacial extent at Mount Rainier National Park from 1896 to 2015*. Natural Resource Report NPS/MORA/NRR—2017/1472. National Park Service, Fort Collins, Colorado.

Dietz, A.J., Kuenzer, C., Gessner, U., and Dech, S. (2012). Remote sensing of snow – a review of available methods, *International Journal of Remote Sensing, 33*(13), 4094-4134, https/doi.org/10.1080/01431161.2011.640964

Domine, F., Albert, M., Huthwelker, T., Jacobi, H.-W., Kokhanovsky, A. A., Lehning, M., Picard, G. And Simpson, W.R. (2007). Snow physics as relevant to snow photochemistry. *Atmospheric Chemistry and Physics Discussions,* 7, pp. 5941–6036.

Dozier, J. (1989). Spectral signature of Alpine snow cover from the Landsat Thematic Mapper. *Remote Sensing of Environment, 28*, 9-22.

Driedger, C., & Kennard, P. (1986). Ice volumes on Cascade Volcanoes: Mount Rainier, Mount Hood, Three Sisters, and Mount Shasta. *U.S. Geological Survey Professional Paper – 1365*.

Goetz, A. F. H. (2012). *Making Accurate Field Spectral Reflectance Measurement*s. ASD Inc., a PANalytical company, Boulder, Colorado, 80301, USA.

Hadley, O., and Kirchstetter, T. W. (2012). Black-carbon reduction of snow albedo. *Nature Climate Change, 2*, 437-440.

Hall, D. K., Riggs, G. A., Salomonson, V. V., Digirolamo, N. E., & Bayr, K. J. (2002). MODIS snow-cover products. *Remote Sensing of Environment, 83*, 181-194.

Jain, S. K., Goswami, A., & Andsaraf, A. K. (2008). Accuracy assessment of MODIS, NOAA and IRS data in snow cover mapping under Himalayan conditions. *International Journal of Remote Sensing, 29*, 563-587.

Kokhanovsky, A. (2013). Spectral reflectance of solar light from dirty snow: a simple theoretical model and its validation. *The Cryosphere, 7*, 1325-1331.

Kunkel, K. E., Robinson, D. A., Champion, S., Yin, X., Estilow, T., & Frankson, R. M. (2016). Trends and extremes in Northern Hemisphere snow characteristics. *Current Climate Change Reports, 2*, 65-73.

Meerdink, S. K., Hook, S. J., Abbott, E. A., & Roberts, D. A. (2018). *The ECOSTRESS Spectral Library 1.0.* Retrieved from https://speclib.jpl.nasa.gov/

Meier, M. F. (1998). *Land ice on Earth: A beginning of a global synthesis.* American Geophysical Union, 19 p.

National Snow and Ice Data Center (NSDIC), (2018). *State of the Cryosphere: Northern Hemisphere Snow.* Accessed June 15, 2018.

Painter, T. H., Rittger, K., Mckenzie, C., Slaughter, P., Davis, R. E., & Dozier, J. (2009). Retrieval of subpixel snow covered area, grain size, and albedo from MODIS. *Remote Sensing of Environment, 113*, 868-879.

Pellika, P., & Rees, W. G. (2010). *Remote Sensing of Glaciers*. CRC Press. London.

Pepe, M., Brivio, P. A., Rampini, A., Nodari, F., & Boschetti, M. (2005). Snow cover monitoring in Alpine regions using ENVISAT optical data. *International Journal of Remote Sensing, 26*, 4661-4667

Rees W. G. (2006). *Remote sensing of snow and ice*. Boca Raton, FL, Taylor and Francis/CRC Press, 285pp. ISBN 0-415-29831-8.

Rutgers University Global Snow Lab. (2017). *Data History*. Retrieved June 15, 2018, from https://climate.rutgers.edu/snowcover/docs.php?target=vis

Takeuchi, N., Dial, R., Kohshima, S., Segawa, T., & Uetake, J. (2006). Spatial distribution and abundance of red snow algae on the Harding Ice field, Alaska derived from a satellite image. *Geophysical Research Letters, 33*(21).

Wang, L., Sharp, M., Brown, R., Derksen, C., & Rivard, B. (2005). Evaluating of spring snow covered area depletion in the Canadian Arctic from NOAA snow charts. *Remote Sensing of Environment, 95*, 453-463.

Warren, S. G. (2013). Can black carbon in snow be detected by remote sensing? *Geophysical Research Letters*, 118, 779-786, doi: 10.1029/2012JD018476.

Xiao, X., Shen, Z., & Qin, X. (2001). Assessing the potential of VEGETATION sensor data for mapping snow and ice cover: A Normalized Difference Snow and Ice Index. *International Journal of Remote Sensing*, *22*(13), 2479-2487.